AURKA/NFκB Axis: A Key Determinant of Radioresistance in Cervical Squamous Carcinoma Cells

Salini Das
Chittaranjan National Cancer Institute
Dilip Kumar Ray
Chittaranjan National Cancer Institute
Elizabeth Mahapatra
Chittaranjan National Cancer Institute
Souvick Biswas
Chittaranjan National Cancer Institute
Madhumita Roy
Chittaranjan National Cancer Institute
Sutapa Mukherjee (sutapa_c_in@yahoo.com)
Chittaranjan National Cancer Institute https://orcid.org/0000-0002-4411-7257

Research Article

Keywords: cervical squamous carcinoma cells, acquired radioresistance, radioadaptive response, AURKA, NFκB signaling

Posted Date: November 30th, 2021

DOI: https://doi.org/10.21203/rs.3.rs-1101050/v1

Abstract

Background: Cervical cancer being one of the leading gynaecological cancers, possess a major threat by its ever-increasing trend of global recurrence events. Radioresistance is one of the major challenges confronted during the treatment of cervical cancer. Radioresistance in cancer cells is manifested by increased rate of cellular proliferation, migration-invasion and cell cycle alterations. Aurora Kinase A (AURKA), a mitotic serine/threonine kinase was found to be overexpressed in cancers and is associated with development of acquired therapy resistance. The principal objective of this study revolved with exploring the mechanisms by which AURKA confers radioadaptive response in cervical cancer cells.

Methods and Results: Parental cervical squamous carcinoma cell line SiHa was subjected to recurrent insult by fractionated dose of X-irradiation. Finally, a resistant subline (SiHa/RR) was isolated at 40Gy. SiHa/RR exhibited higher expression of AURKA/ pAURKA along with the signaling molecules that are favored by this kinase (HIF1α, pAkt, NFκB) vis-à-vis lower expressions of the molecules that are generally suppressed by AURKA (p53, Gadd45a). Surprisingly, inhibition of AURKA in SiHa/RR showed improved radiosensitivity by reducing the wound healing capacity, sphere forming ability and enhancing radiation induced apoptosis. Ectopic overexpression of AURKA gave rise to radioresistant phenotype in parental SiHa by stimulating nuclear translocation of NFκB. This pattern of increased nuclear localization of NFκB was also observed in resistant subline as a consequence of activation and overexpression of AURKA.

Conclusion: These findings strengthened the involvement of AURKA in radioresistance via activating NFκB mediated signaling pathway to deliver radioresistant associated adaptive complexities.

Introduction:

Cervical cancer prevails as one of the leading gynaecological cancers for its higher incidences and mortality [1, 2]. Therapeutic success might be achieved against cervical cancer at early stage of diagnosis, primarily by surgery or radiation [3]. The metastatic form of carcinoma is yet a challenging regimen that seeks urgent attention to explore novel therapeutic approaches. Cervical cancer has a global moderate to high recurrence rate throughout the stages after the initial treatment because of survival of cancer cells despite the radiation therapy that causes disease relapse [4]. Understanding the underlying strategies of these surviving cells is an urgent need of the hour. Most of the time, the efficacy of radiation therapy depends on the phases of cell cycle. The relative radiosensitive response of a cell becomes highly active at the G2/M phase making the G2/M arrest the master-strategy of radiation induced killing of cells [5, 6]. Alteration in the cell cycle pattern is therefore a key to achieve radioresistance.[7] Aurora Kinase A (AURKA) is a well characterized mitotic serine threonine kinase, predominantly accountable for G2/M progression of cell cycle [8]. Conventionally AURKA promotes proper mitotic exit, stabilization of centrosome, proper formation of spindle as part of its canonical mitotic role [9]. Moreover, involvement of AURKA is also evident in the development of acquired chemoresistance in several cancers [10]. Radioresistance is predominantly caused by accumulation of altered characters within and is manifested by reshaping the cellular behavior such as its hyper proliferative capability, obtaining EMT phenotype and

induction of stemness within them [11]. Previous researches proposed AURKA as a key contributor of radioresistance; yet the underlying mechanisms need elucidation [12, 13]. Therefore, understanding AURKA mediated signaling pathway in radioresistant scenario may put forward opportunities for exposure of new domains of molecular therapy. The present study has been taken up to find out the actual adaptive features gained during chronic cumulative irradiation at the cellular level. Hence attempts were undertaken to develop and characterize radioresistant cervical cancer cell line via fractionated irradiation. Successive molecular assays were carried out in order to explore concomitant cellular adaptability and AURKA mediated signaling complexities required for imparting radioresistance; where NFκB mediated activation of prosurvival pathway was found to be favored by AURKA.

Materials And Methods:

Chemical reagents:

The primary antibodies used for the study, anti-p53, anti-phospho-Akt(S473), anti- FITC-conjugated anti-rabbit IgG were purchased from Genetex, CA, USA. An antibody against Aurora A was purchased from Biolegend. β-actin antibody was procured from abcam, Cambridge, UK. Anti-NFκB p50, p65, anti-Ki67, anti-PCNA, anti-MMP9 and anti-Oct 4 antibodies were obtained from Santa Cruz USA. Antibodies against phospho-Aurora(T288) and GADD45α were procured from Cell Signaling Technology, USA. Trypan Blue, PI (Propidium Iodide), DAPI (4',6-diamidino-2-phenylindole), Aurora-A Inhibitor I or AKI and BSA (Bovine Serum Albumin) were purchased from Sigma-Aldrich, USA. All other reagents of analytical grade were procured locally.

Cell lines and cell culture:

Human cervical squamous carcinoma cell line SiHa was obtained from National Centre for Cell Science (NCCS), Pune INDIA. Subsequently a radioresistant subline SiHa/RR was developed by weekly incremental fractionated doses of irradiation. Cells were maintained in each irradiated dose for 5 passages and finally a colony was isolated at 40 Gy; designated as SiHa/RR. Both SiHa and SiHa/RR cells were maintained in MEM supplemented with 15% heat inactivated fetal bovine serum (FBS) and antibiotics (gentamycin 40 µg, penicillin 100 units, streptomycin 10µg/ml). Cells were maintained at 37^0C in a humidified CO_2 incubator having 5% CO_2/95% air.

Irradiation:

SiHa cells were initially, cultured to reach an approximate confluence of 50% in 25 cm^2 cell culture flasks (Greiner Bio-One International). The culture medium was replenished with 2 ml of fresh complete MEM 15 min prior to administration of radiation dose. Flasks were then irradiated using X-Ray linear accelerator (Elekta). Medium of the post-irradiated cultured flask was replaced with 5 ml fresh medium before further incubation. Surviving cells were allowed to repopulate until reaching maximum confluency and then again subcultured into two new flasks after proper trypsinization. Upon attaining 50% confluency, these cells were subjected to another round of irradiation in the following week. The initial

dose of irradiation being 2 Gy, successive weekly incremental doses of 0.5 Gy was administered for 15 weeks to achieve total cumulative dose of 40 Gy. A weekly maintenance dose of 2 Gy was continued to the cultured flask of finally isolated subline for sustaining adaptability of the cells. Further experiments were accomplished with exponentially growing cells after 48 h of the last maintenance irradiation.

Morphological observation and cell viability assay

SiHa and SiHa/RR cells were examined under Phase contrast microscope (Carl ZEISS) at the magnification of 400X. Images were captured and analyzed (Nucleus: Cytoplasm) using FIJI software. The alterations in the ratio were plotted graphically. Roughly $1x10^5$ cells were seeded into a 25 cm^2 flask (Greiner Bio One International) 48 h prior to the first irradiation. These cells were weekly exposed to previously mentioned doses of X-Ray. Cells were trypsinized 1 h after each irradiation and single suspended cells were counted using haemocytometer after staining with Trypan Blue for 15 min (Sigma). Unstained (viable) and stained (nonviable) cells were counted separately in the hemacytometer and percentage of viable cells were calculated as total number of viable cells / total number of cells X 100 and were calculated and plotted graphically for assessment.

Clonogenic viability assay:

Confirmation of acquired radioresistance was evaluated by the ability of colony formation upon challenging with acute radiation dose in both SiHa and SiHa/RR. Cells at a number of 1000 per well was seeded in 96-well plate. After 24 h of incubation, both SiHa and SiHa/RR cells were irradiated with an acute dose of 10Gy. Cellswere allowed to grow further till visible colonies were found. Colonies were subsequently stained with 0.5% crystal violet (Sigma, St. Louis, MO) and colonies of 50 cells or more were counted under microscope. Surviving fraction (SF) was calculated as percentage of number of colonies formed to total number of seeded cells. This set of experiment was furthermore repeated with pretreatment withaspecific Aurora Kinase Inhibitor I orAKI (0.01μM for 24 h) prior to exposure to acute 10Gy radiation dose.

Flow cytometric analysis:

Cell Cycle phase specific distribution of parental vs. radioresistant cells was evaluated using flow cytometry technique following standard laboratory protocol [14]. Both SiHa and SiHa/RR cells were treated with 10Gy of acute X- irradiation. After 6 h of treatment, $2x10^6$ cells were suspended in cold PBS and centrifuged at 100 g for 8 min. Successive fixation of cells were done in 70% cold absolute ethanol for keeping under incubation in ice for 30 min. Cell pellets obtained after centrifugation and removal of ethanol were suspended in 1ml DNA binding solution (200 μg/ ml RNase + 50 μg/ml PI). Prior to analysis in Thermo Fisher Flow Cytometer, cell suspension in this condition was kept at dark for 30 min. Fluorescence was captured on BL2A channel and 10,000 cells with logarithmic amplification were counted. Percentage of AURKA expressed cells were determined flow-cytometrically by staining the acetone fixed SiHa and SiHa/RR cells with AURKA antibody tagged with Alexa Fluor 488 (Novus Biologicals) and Fluorescence was captured on BL2A channel.

Immunoblotting technique:

Protein expression was determined by standard laboratory technique of immunoblotting [15]. Briefly, 6 h post irradiated (10Gy) SiHa/RR as well as parental radiosensitive SiHa cells were harvested and cell lysates were prepared using lysis buffer. Additionally in another set, SiHa/RR cells were pretreated with AKI (24h) followed by 10 Gy irradiation with an incubation for 6 h followed by cell lysates preparation. Proteins were quantitated by Bradford colorimetric assay. Electrophoresis (Bio-Rad apparatus) of equal amounts of total proteins were performed on SDS-polyacrylamide gel using electrophoresis buffer (Tris: 25 mM, glycine: 192 mM, SDS: 20%) and electro-transferred to nitrocellulose membranes using transfer buffer (Tris: 250 mM, glycine: 192 mM, methanol: 10%). Membranes were blocked in 5% BSA; thereafter incubated overnight with respective primary antibodies at 4^0C. Following incubation, membranes were washed with TBST (Tris Buffered Saline with Tween20) thrice and further incubated with alkaline phosphatase-conjugated anti-mouse IgG or anti-rabbit IgG (1:1000 dilutions in TBS). TBST was used for subsequent washing of membranes for removal of nonspecific binding of secondary antibodies. Proteins were thereafter visualized upon addition of BCIP/NBT in the form of colorimetric bands. The comparative expression profiles of Ki-67, PCNA, AURKA, p53, Gadd45α HIF1 α, NFκB p50, NFκB p65, Akt, phospho Akt, MMP, Oct4 was assessed using β-actin as loading control.

In silico clustering analysis:

String Database was used to study the interactions between the proteins which were found to be overexpressed in SiHa/RR cells based on the formula Network analysis = Network Enrichment Analysis + Network Topological Analysis.

In Vitro Scratch (migratory) assay:

Alteration of cell motility was determined using *in vitro* scratch or migratory assay. A scratch was drawn in a straight line over the monolayer of the confluent culture using 200µl sterile pipette tip. The treatment conditions were **a).** Untreated SiHa cells, **b).** 6 h post irradiated cells (10Gy acute shot) and **c).** Cells pretreated with AKI (0.01 µM) for 24 h followed by 10Gy X-irradiation and subsequent incubation for 6 h. The image of the scratch width was captured under a phase-contrast microscope, immediately after treatment (0 h) and again after 36 h of incubation. Percentage of wound healing area was determined by calculating the reduction of the scratch-width (width of the space devoid of migrating cells) after the indicated incubation time and expressed as percentage of wound closure. Scratch area was calculated using FIJI software.

3D sphere formation Assay:

3D sphere forming assay was carried out using hanging drop method as described by Foty with slight modifications [16]. Treatment conditions were similar to that of wound healing assay. Following completion of treatment, cells were trypsinized and resuspended in the medium. The lid of a 60 mm tissue culture plate was removed and inverted to deposit 10 µl drops onto the bottom of it using 20 µl

pipett (up to 20 drops were placed in well maintained distance from each drop). The lower plate was filled with 5 ml of sterile PBS to use it as a hydration chamber. The PBS-filled chamber was covered by the lid containing cell droplets. Such plates were kept for incubation at 37^0C/5% CO_2 with95% humidity till visible cell sheets or aggregates were found on the lid. After microscopical confirmation of conspicuous cell sheets, those were transferred to 25 cm^2 flasks filled with 3 ml complete medium and were placed in shaker incubator at 37^0C and 5% CO_2 till the development of spheroids. Microscopic observation and capturing of image were performed at the 100X magnification using a phase contrast microscope (Zeiss). Further measurement of sphere area was performed using FIJI software.

Apoptotic assay:

To examine the characteristic morphological features of apoptosis, bothSiHa and SiHa/RR cells were exposed to acute shot (10 Gy) of irradiation. Cells were harvested, 6 h after irradiation, washed with PBS and centrifuged and to the pellet PI (Sigma-Aldrich) was added (final: 50µg/ml). AKI pretreated cells (as described in earlier experimentations) were also stained with PI. Cells were then incubated in the dark at RT for 10 min. Both treated and untreated cells were smeared in the glass slide, covered with cover slip, and observed under the fluorescent microscope. Characteristic apoptotic cells were examined under a fluorescence microscope at PI specific filter (Leica).

Ectopic overexpression of AURKA using plasmid DNA:

Confluent SiHa cells were added with specific plasmid with the modified pcDNA5/FRT/TO vector containing a single amino-terminal Myc tag and the human wild type AURKA transgene (Plasmid #59804; pcDNA5 FRT TO Myc ArA WT, AddGene) and lipofectamine to Opti-MEM aliquots (250 µl each) and incubated for 5 min at room temperature. Thereafter, plasmid/Opti-MEM and the Lipofectamine 3000/Opti-MEM was mixed and allowed to incubate for 20 mins at room temperature. Plasmid containing medium was added to cells in culture. Finally, expression was checked by western blotting and immunofluorescence assay.

Statistical Analysis:

Comparative analysis of differences between groups was carried out using Student's t test in the GraphPad Prism 5.0 software package (GraphPad Software, Inc., La Jolla, CA, USA). $p<0.001$ was considered the minimal level of significance. Data or values were obtained from at least three independent experiments and expressed as Mean ± SD.

Results:

Confirmation and Characterization of radioresistant subline SiHa/RR:

To perceive the role of AURKA in radioresistance, a radioresistant cervical squamous cell carcinoma cell line (SiHa/RR) was developed by subjecting parental SiHa cell to weekly fractionated dose of X-ray with

an initial dose of 2Gy followed by a weekly incremental dose of 0.5 Gy. Finally, the subline was isolated at a cumulative dose of 40 Gy **(Fig 1a)**. Isolated radioresistant subline was further maintained at a steady state weekly radiation of 2 Gy. For confirming the features associated with radioresistance, further experimentations were carried out by irradiating both parental and resistant cells with acute doses of 2, 4, 6, 8 and 10Gy. In order to ascertain acquirement of radioresistant property, SiHa/RR cells were seeded to examine their colony formation ability with SiHa as control. It was observed that SiHa/RR cells showed intensified survival fractions with increased percentage of colony forming ability compared to radiosensitive parental SiHa. Furthermore, exposure to acute dose of 10Gy resulted into enhanced colony formation in SiHa/RR cells. Contrarily, parental SiHa showed radiosensitive response by reducing survival fraction and with lesser number of formations of colonies upon exposure to similar dose (10Gy) of acute radiation (**Fig 1b**). The surviving fraction as calculated by the ratio of number of colonies to total number of cells seeded x100, showed consistent resistance to radiation in SiHa/RR cells (**Fig 1c**). Based on these preliminary observations it was felt curious to look into the morphological changes if any occurs within SiHa/RR cells. Phase Contrast microscopic study at the magnification 400X exhibited enlarged nuclei in SiHa/RR cells with increased Nucleus to Cytoplasmic (N/C) ratio. N/C ratio as observed in SiHa (1:3) was found to increase significantly (4:1) in radioresistant SiHa/RR cells (**Fig 1d, e**). To further explore the underlying association between increased nucleo-cytoplasmic ratio with drastic elevation in the number of colonies, expression patterns of proliferative markers PCNA and Ki67 was looked into by western blot analysis. Immunoblot data indicated augmented expressions of both of the markers in SiHa/RR; denoting higher proliferative capacity of SiHa/RR cells. Such ability may be achieved due to acquirement of radio-adaptive response. Corresponding band intensities were calculated using ImageJ software and represented graphically which were in coherence with survival fraction and morphological changes as observed in SiHa/RR cells **(Fig 1f**). Based on these findings, attempts were made to look over the doubling time of SiHa/RR. Using the slope of log phased cells as plotted in the graph (**Fig 1g**), it was noticed that the doubling time of parental SiHa was 33 h while that of SiHa/RR was shortened to24 h; indicating enhanced proliferating potential upon acquirement of radioresistance. Additionally, parental SiHa upon exposure to chronic fractionated dose of X-Ray during development of radioresistant subline showed an initial response to irradiation as percentage of cells were dropped down to 60% after 4Gy irradiation. With subsequent gradual incremental doses, the percentage of cell viability restored gently particularly from 12Gy onwards and reached a plateau at 16Gy. This finding was suggestive of cellular adaptability of SiHa cells upon chronic exposure to irradiation (**Fig 1h**).

Elevated AURKA level protects radioresistant subline SiHa/RR from radiation induced G2/M arrest

Alteration in the Cell cycle phase distribution between SiHa and SiHa/RR was assessed using flow cytometer. SiHa and SiHa/RR cells at 0 and 10Gy of acute radiation doses were harvested 6 h after irradiation and finally stained with DNA binding solution containing propidium iodide. The result analysed at BL2A propidium iodide specific filter, displayed higher proportion of arrest of SiHa cells at G2 phase upon exposure to acute dose of 10Gy radiation. Contrarily, SiHa/RR exhibited significantly lower proportion of G2/M cells; even after same dose of exposure. This Flow cytometric analysis as performed by Cytospec Software (**Fig 2a**) and graphical representation of phase wise distribution of cells **(Fig 2b**),

indicated that SiHa/RR cells efficiently escaped from the radiation induced cell cycle arrest and led to significant ($p < 0.0001$) progression from G2 to M phase. Values obtained were Mean ± SD of three independent experiments. The percentage of AURKA positive cells were calculated furthermore which was higher in SiHa/RR particularly after irradiation in comparison to radiosensitive SiHa cells (**Fig 2c**). The proliferative and survival mode of the radioresistant cells made the investigators curious to find the differential expression pattern AURKA in radioresistant and sensitive cells along with its effectors. Western blot analysis revealed overexpression of AURKA particularly phospho-AURKA (T288) in SiHa/RR in absence or even more in presence of acute irradiation. Such an elevated expression of active form of AURKA substantiated the conviction of its contribution in development of radioresistant phenotype. HIF1α, a key orchestrator of radioresistance and an upstream regulator of AURKA was looked furthermore. Radiation induced HIF1α was clearly visible in SiHa, whereas a trend of overexpression pattern of the same was observed in SiHa/RR. Since activated AURKA phosphorylates Akt at S473, expression of Akt and phospho Akt were looked into. The observed trend showed surged expressions of total Akt, phospho Akt (S473) and their downstream molecules NFκB(both p50 and p65) in SiHa/RR in comparison to SiHa (**Fig 2d**). Expression status of DNA damage regulator proteins like p53 and Gadd45α were reduced surprisingly in SiHa/RR. The existence of any interactive association between the proteins with altered expression in SiHa/RR was examined by String Database which indicated a prominent relationship between AURKA, NFκB, p53, Gadd45α, HIF1α notifying a possible signaling mechanism favouring the radioresistance in SiHa/RR (**Fig 2e**).

Inhibition of AURKA reinstates radiosensitivity by reversing radioadaptive response in SiHa/RR cells:

To establish the mediatory role of AURKA in colony forming ability of cells, both SiHa and SiHa/RR cells were pretreated with Aurora A Inhibitor I (0.01 μM) for 24 h and then subjected to acute dose of irradiation of 10Gy with subsequent post incubation for 6 h. It was obvious from the result that the pretreatment with AURKA inhibitor increased the radio sensitivity of SiHa/RR by reversing radioresistance as revealed from the clonogenic assay (**Fig 3a)**. Calculation of survival fraction was also in alignment with the number of colonies formed (**Fig 3b)**, where marked reduction in the clonogenic survival rate ($p<0.001$ compared to untreated cells) at 10Gy dose was apparent. Next the rate of radiation induced apoptosis was measured in both SiHa and SiHa/RR in untreated vs. acute irradiation (10 Gy). Cells were stained with fluorescent dye propidium iodide. Untreated cells showed a relatively uniformly stained nucleus with no visible damage to nuclei. Whereas upon exposure to 10Gy irradiation SiHa exhibited characteristic morphological features of apoptotic cells when observed under the fluorescent microscope. Some of the notable apoptotic features with higher frequencies of fragmented nuclei were found in SiHa (**Fig 3c**). SiHa/RR on the contrary failed to undergo apoptosis upon 10Gy irradiation. Nonetheless treatment of SiHa/RR with Aurora A Inhibitor I prior to acute shot of irradiation sensitized cells to undergo radiation induced apoptosis; confirming implication of AURKA in developing radioadaptive response to escape apoptosis (**Fig 3c**). To check whether SiHa/RR cells have developed the traits of increased cell migration and invasion ability, 2D scratch assay was performed. Wound healing assay or scratch assay revealed that SiHa/RR had the ability of remarkably faster closure rate of wound area compared with SiHa (**Fig 3d**). Cell migration of SiHa/RR cells was found to be increased by 60%, when compared with

control SiHa (**Fig 3d**). It was observed that prior administration of AURKA inhibitor remarkably prevented the wound closure ability of SiHa/RR cells by obstructing its migratory capacity. This result clearly advocated the involvement of elevated expression of AURKA in mediating radioresistant phenotype by increasing migratory potential of the SiHa/RR cells. Since development of stemness is frequently correlated with metastasis, western blot analysis was performed further. Upregulated expression of stemness marker Oct4 in SiHa/RR cells were significantly reduced upon pretreatment with AURKA inhibitor. Similar trend in expression pattern of metastatic marker MMP9 was documented from the result (**Fig 3e**). This result justified the attribution of AURKA in development of radioresistance by inducing stemness and metastasis in radioresistant subline SiHa/RR. Sphere forming assay revealed development of nonadherent spherical clusters of cells particularly in SiHa/RR; one week after cell seeding in anchorage independent condition. These results justified the previous findings of better migration and invasion property in radioresistant SiHa/RR cells. To further establish the possible involvement of AURKA in acquirement of radioadaptive response, by increased migration and proliferation potential, both SiHa and SiHa/RR were treated with Aurora A Inhibitor I at a dose of 0.01 μM for 24 h followed by acute radiation shot of 10Gy. Sphere forming ability of both SiHa and SiHa/RR was reduced significantly (**Fig 3f**). Fold increase in sphere area was calculated using FIJI software. The graphical result (**Fig 3g**) clearly corroborated with the microscopic findings.

Blocking of AURKA in radioresistant subline hinders nuclear translocation of NFκB:

Expression and intracellular localization of AURKA was detected after treating SiHa/RR cells with AKI by Immunofluorescent study (**Fig 4a**). Microscopic images disclosed conspicuous localization of AURKA at the centrosome of SiHa/RR compared to SiHa cells. Upon treatment with AKI reduced centrosomal localization of AURKA was noted (**Fig 4a**). In corroboration with the western blot findings of upregulated NFκB expression, further experimentation was carried out to establish the involvement of AURKA in nuclear localization of NFκB. Immunofluorescence study in presence of AKI diminished expressions of both p65 and p50 subunits (**Fig 4b, c**). To strengthen this observation, western blot analysis of NFκB (p50 and p65)was re-performed using nuclear extract of SiHa/RR cells upon treatment with AKI. The expression of NFκB was effectively reduced as a result of AURKA inhibition (**Fig 4d**). These observations clearly highlighted a strong positive correlation (Correlation coefficient: 0.97) between AURKA inhibition with hindered nuclear translocation of NFκB.

Ectopically overexpressed AURKA promotes radioadaptive responses in SiHa cells by triggering nuclear translocation of NFκB

The striking restoration of radiosensitivity in SiHa/RR cells upon AURKA inhibition encouraged to explore whether ectopic overexpression of AURKA in parental SiHa cells could indeed impart radioresistance in SiHa cells. To achieve this goal, SiHa cells were transfected with AURKA plasmid. The overexpression of AURKA in SiHa cells were confirmed by using western blot (**Fig 5a**) and immunofluorescence assay (**Fig 5b**). Further its effect in radioresistance was evaluated by exposing these cells to 2, 4, 8, 10 Gy of radiation and corresponding clonogenic viability assays were performed to

get the survival fraction. Results indicated higher survival fractions in AURKA overexpressed SiHa cells (**Fig. 5c, d**);suggesting an enhanced proliferating ability. Further, the metastatic potency of the cells was investigated by sphere forming assay. SiHa cells when overexpressed with AURKA showed increased sphere area compared to control SiHa (**Fig. 5e**). Since a major difference in cell cycle was observed between SiHa and SiHa/RR particularly at the G2/M population, flow cytometric analysis of cell cycle was performed in AURKA overexpressed SiHa cells. The data revealed a similar trend of reduced G2/M population in the transfected SiHa cells even at the acute exposure of 10 Gy radiations (**Fig. 5f, g**). To further look insight the AURKA mediated loss of radiosensitivity with acquirement of radioadaptive response, the expression status of NFκB and its nuclear localization in the transfected cells were examined by western blot and immunofluorescence study. SiHa with AURKA overexpression displayed prominent nuclear localization and overexpression of NFκB in nuclear extract of transfected cells (**Fig 5h, i**); which clearly affirmed the notion of AURKA mediated functional activation of NFκB. Based on these findings further experimentations related to apoptotic ability of AURKA overexpressed cells were performed. Morphological observation of PI stained AURKA overexpressed cells were found to have much lesser apoptotic nuclei upon irradiation (**Fig 5j**). Collectively, these findings asserted the involvement of in delivering radioresistant phenotype in SiHa cells.

Discussion:

The primary purpose of this study was to simulate the cells found in the radioresistant tumour microenvironment and to investigate the involvement of AURKA in imparting radioresistance in cervical cancer cells. Since the invasive carcinoma in cervix occurs at the squamo-columnar junction, cervical squamous carcinoma cell was used for the study. Building a radioresistant cell subline SiHa/RR was accomplished upon fractionated irradiation to the parental cervical squamous carcinoma cell SiHa. Chronic irradiation contributed in acquirement of radioadaptive alterations in SiHa/RR particularly in case of increased N/C ratio, overexpression of proliferative markers (PCNA, Ki67), improved survival fraction and viability as found from the trypan blue viability assay and clonogenic viability assay. The significant reduction in doubling time of (24 h in SiHa/RR instead of 33 h as found in SiHa), with an indication of faster proliferation rate made the investigators curious to find any difference in cell cycle pattern in SiHa/RR compared to SiHa. Since the effectivity of radiation depends on the phases of cell cycle, the strategy of radioresistant cells involve adjusting the cell cycle pattern in response to irradiation [17]. The increased G2/M population in SiHa cells is indicative to its radiosensitivity, as radiation cause G2/M arrest for effective killing of cells. On the contrary, SiHa/RR showed reduced G2/M population emphasizing the potential ofovercoming the G2/M arrest, which enabled SiHa/RR cells to continue cell cycle progression. Therefore, the possibility of interference of any mitotic kinase in radioresistance was strengthened from the observations. To address the notion, expression level of AURKA was carried out by western blotting and flow cytometric analysis. SiHa/RR showed AURKA overexpression even at the per cell specific expression level. Results not only revealed the overexpression of AURKA but also its over-activation in SiHa/RR as activated form of AURKA (pAURKA: T288) was simultaneously overexpressed [18]. Further, the expression status of some of the downstream signaling molecules like Akt and its

activated form phospho Akt (S473; which is a site of phosphorylation mediated by AURKA) [19], NFκB (p50 and p65) was found to be overexpressed in SiHa/RR. On the contrary, protein level of DNA damage markers like p53, Gadd45α was downregulated. Studies have disclosed that AURKA lowers the expressions of p53 by regulatory phosphorylation at S215 and S315 residues, which in turn facilitates p53 degradation via MDM2 mediated ubiquitination [20]. Downregulated expression of p53 and GADD45α as notable from the present findings possibly promoted G2/M progression as both the molecules cause cell cycle arrest in response to radiation induced DNA damage [21, 22]. To ascertain the contributory role of AURKA as a mediator of radioresistance, clonogenic survival assay was performed in the presence and absence of AURKA inhibitor. SiHa/RR while treatment with AKI showed a notable reduction in the number of colonies compared to the untreated cells. This observation helped to progress further to find the likelihood of AURKA in attainment of radioadaptive alterations in SiHa/RR. String interaction results indicated interplay of signaling molecules of AURKA pathway in SiHa/RR. AURKA was found to be strongly interacted with p53, Gadd45a, Akt and PCNA and NFκB [23-25]. Hyper-proliferative potential of SiHa/RR aided in increased migration and invasion capabilities as found from the result of wound healing assay where SiHa/RR filled the gap at a much faster rate compared to SiHa. The 3D spheroid forming ability was increased in SiHa/RR as measured by the increased sphere area. The subsequent reduction in wound healing property and sphere forming capacity in SiHa/RR upon treatment with AKI made the possibility stronger that AURKA helped in the induction of stemness and metastasis in the radioresistant cells. Owing to this the expressions of Oct4 and MMP9; two known markers of stemness and EMT as well as downstream effector of NFκB [26, 27] were examined by western blot analysis in the presence and absence of AKI for venturing the role of AURKA in the induction of EMT and stemness in SiHa/RR. Radiation mediated acquisition of radioresistance was previously explained and reported by other investigators by the induction of epithelial-to-mesenchymal transition (EMT); a notable phenotypic and molecular alterations [27-29]. These present observations further reinforced AURKA mediated acquisition of radioresistance with development of more mesenchymal like phenotype along with increased potential of invasion and migration in SiHa/RR cells. Both of these molecules were overexpressed in SiHa/RR but got downregulated upon administration of AKI. Finally, apoptotic results further affirmed lesser responsiveness of SiHa/RR towards apoptosis as revealed from the results obtained from Propidium iodide staining. Increased radiosensitivity was further documented by increasing the radiation induced apoptosis potential upon treatment with AKI. The principal mechanism in imparting radioresistance mediated by AURKA was activation of prosurvival pathway via facilitating nuclear localization of NFκB as evident in SiHa/RR as well as in SiHa transfected with AURKA plasmid. The enhanced expression of NFκB in the nuclear fraction strengthens this notion both in radioresistant subline and transfected subline. These observations are in agreement with some of the previous findings where AURKA with other downstream signaling axis showed significant contribution in acquisition of radioresistance in cancer [30-35] Overexpression of AURKA coincided with the acquired features of SiHa/RR which justified the hypothesis of involvement of AURKA as a mediator to acquire radioadaptive response in cervical cancer cells for the attainment of radioresistance by promoting nuclear translocation of NFκB.

Conclusions:

Accumulation of radioadaptive response within cells in response to chronic administration of incremental doses of radiation, as revealed from the present findings generated several survival approaches via tuning the existing molecular scenario, especially triggering the expression of prosurvival molecules and overcoming necessary arrest to minimize the chances of apoptotic stimulation. Interestingly these alterations generated in course of radioresistance coincide with majority of the functional activities of AURKA including cell proliferation, migration, invasion, epithelial-mesenchymal transition (EMT) and maintenance of cancer stem cell (CSC) behaviors and led to anticipate AURKA as one of the prime mediators of radioresistance in cancer. This work therefore provides an access to a new horizon of further investigations to establish AURKA not only as a biomarker but also an essential therapeutic target to combat radioresistance.

Declarations

Acknowledgement:

The authors are indebted to **Director CNCI** for providing the necessary infrastructural facilities. The authors expressed whole hearted gratifications to **Pijus Kanti Ghosh and team** for their technical help from the **Department of Medical Physics, CNCI, Kolkata, India**.

Funding:

This work was supported by Council of Scientific and Industrial Research (CSIR), Government of India by providing fellowship and contingency grant, as a part of PhD project.

Competing Interests:

The authors have no financial or non-financial interest to disclose

Author's contribution:

Primary experimentation, Data collection and analysis and manuscript preparation was performed by **Ms Salini Das** and this work is a part of her Ph.D project. **Dr. Dilip Kumar Ray** provided his valuable help in calculating radiation dose and guiding in the irradiation procedures. **Ms Elizabeth Mahapatra** and **Mr. Souvick Biswas** had performed part of the experimentations and had helped in data analysis. **Dr. Madhumita Roy** had contributed her valuable insights in data processing. The entire project was designed by **Dr. Sutapa Mukherjee** who had offered her sincere interests in all the work plans, data analysis and processing of manuscript.

Ethical approval

None

Informed consent

None.

Consent to participate

All authors have confirmed their participation in this study.

Consent to publish

All authors have agreed to publish this manuscript.

References

1. Arbyn M, Weiderpass E, Bruni L, de Sanjosé S, Saraiya M, Ferlay J, Bray F (2020) Estimates of incidence and mortality of cervical cancer in 2018: a worldwide analysis. The Lancet Global health 8(2):e191–e203
2. Sung H, Ferlay J, Siegel RL, Laversanne M, Soerjomataram I, Jemal A, Bray F (2021) Global cancer statistics 2020: GLOBOCAN estimates of incidence and mortality worldwide for 36 cancers in 185 countries. Cancer J Clin 71(3):209–249
3. Denny L (2012) Cervical cancer: prevention and treatment. Discov Med 14(75):125–131
4. Tyagi A, Vishnoi K, Kaur H, Srivastava Y, Roy BG, Das BC, Bharti AC (2017) Cervical cancer stem cells manifest radioresistance: Association with upregulated AP-1 activity. Sci Rep 7(1):1–14
5. Pawlik TM, Keyomarsi K (2004) Role of cell cycle in mediating sensitivity to radiotherapy. International Journal of Radiation Oncology* Biology* Physics 59(4):928–942
6. Dillon MT, Good JS, Harrington KJ (2014) Selective targeting of the G2/M cell cycle checkpoint to improve the therapeutic index of radiotherapy. Clin Oncol 26(5):257–265
7. de Jong Y, Ingola M, Briaire-de Bruijn IH, Kruisselbrink AB, Venneker S, Palubeckaite I, Bovée JV (2019) Radiotherapy resistance in chondrosarcoma cells; a possible correlation with alterations in cell cycle related genes. Clinical sarcoma research 9(1):1–11
8. Liu X, Zhang Y, Wu S, Xu M, Shen Y, Yu M, Ye X (2020) Palmatine induces G2/M phase arrest and mitochondrial-associated pathway apoptosis in colon cancer cells by targeting AURKA. Biochem Pharmacol 175:113933
9. Nikonova AS, Astsaturov I, Serebriiskii IG, Dunbrack RL, Golemis EA (2013) Aurora A kinase (AURKA) in normal and pathological cell division. Cell Mol Life Sci 70(4):661–687
10. Biswas S, Mahapatra E, Ghosh A, Das S, Roy M, Mukherjee S (2021) Curcumin rescues doxorubicin responsiveness via regulating Aurora a signaling network in breast cancer cells. Asian Pac J Cancer Prev 22:957–970
11. Lee SY, Jeong EK, Ju MK, Jeon HM, Kim MY, Kim CH, Park HG, Han SI, Kang HS (2017) Induction of metastasis, cancer stem cell phenotype, and oncogenic metabolism in cancer cells by ionizing

radiation. Mol Cancer 16:10

12. Liu F, Zhang Y, Dong Y, Ning P, Zhang Y, Sun H, Li G (2021) Knockdown of AURKA sensitizes the efficacy of radiation in human colorectal cancer. Life Sci 271:119148
13. Oh ET, Byun MS, Lee H, Park MT, Jue DM, Lee CW, Lim BU, Park HJ (2010) Aurora-a contributes to radioresistance by increasing NF-kappaB DNA binding. Radiat Res 174:265–273
14. Sarkar R, Mukherjee S, Roy M (2013) Targeting heat shock proteins by phenethyl isothiocyanate results in cell-cycle arrest and apoptosis of human breast cancer cells. Nutr Cancer 65:480–493
15. Souvick B, Elizabeth M, Madhumita R, Sutapa M (2020) PEITC by regulating Aurora Kinase A reverses chemoresistance in breast cancer cells. Indian Journal of Biochemistry and Biophysics (IJBB) 57(2):167–177
16. Foty R (2011) A simple hanging drop cell culture protocol for generation of 3D spheroids. J Vis Exp 51:2720
17. Otani K, Naito Y, Sakaguchi Y, Seo Y, Takahashi Y, Kikuta J, Ishii M (2016) Cell-cycle-controlled radiation therapy was effective for treating a murine malignant melanoma cell line in vitro and in vivo. Sci Rep 6(1):1–8
18. Janeček M, Rossmann M, Sharma P, Emery A, Huggins DJ, Stockwell SR, Venkitaraman AR (2016) Allosteric modulation of AURKA kinase activity by a small-molecule inhibitor of its protein-protein interaction with TPX2. Sci Rep 6(1):1–12
19. Dar AA, Belkhiri A, El-Rifai W (2009) The aurora kinase A regulates GSK-3β in gastric cancer cells. Oncogene 28(6):866–875
20. Du R, Huang C, Liu K, Li X, Dong Z (2021) Targeting AURKA in Cancer: molecular mechanisms and opportunities for Cancer therapy. Mol Cancer 20(1):1–27
21. Kleinsimon S, Longmuss E, Rolff J, Jäger S, Eggert A, Delebinski C, Seifert G (2018) GADD45A and CDKN1A are involved in apoptosis and cell cycle modulatory effects of viscumTT with further inactivation of the STAT3 pathway. Sci Rep 8:5750
22. Singh SK, Banerjee S, Acosta EP, Lillard JW, Singh R (2017) Resveratrol induces cell cycle arrest and apoptosis with docetaxel in prostate cancer cells via a p53/ p21WAF1/CIP1 and p27KIP1 pathway. Oncotarget 8:17216–17228
23. Sánchez R, Pantoja-Uceda D, Prieto J, Diercks T, Marcaida MJ, Montoya G, Campos-Olivas R, Blanco FJ (2010) Solution structure of human growth arrest and DNA damage 45alpha (Gadd45alpha) and its interactions with proliferating cell nuclear antigen (PCNA) and Aurora A kinase. J Biol Chem 285:22196–22201
24. Chowdhury P, Perera D, Powell RT, Talley T, Tripathi DN, Park YS, Dere R (2021) Therapeutically actionable signaling node to rescue AURKA driven loss of primary cilia in VHL-deficient cells. Sci Rep 11(1):1–13
25. Miralaei N, Majd A, Ghaedi K, Peymani M, Safaei M (2021) Integrated pan-cancer of AURKA expression and drug sensitivity analysis reveals increased expression of AURKA is responsible for drug resistance. Cancer Med 10(18):6428–6441

26. Fan X, Zhou J, Bi X, Liang J, Lu S, Yan X, Luo L, Yin Z (2021) L-theanine suppresses the metastasis of prostate cancer by downregulating MMP9 and Snail. J NutrBiochem 89:108556
27. Tahmasebi-Birgani MJ, Teimoori A, Ghadiri A, Mansoury-Asl H, Danyaei A, KhanbabaeiH (2018) Fractionated radiotherapy might induce epithelial-mesenchymal transition and radioresistance in a cellular context manner. J Cell Biochem 120:8601–8610
28. Jin Y, Xu K, Chen Q, Wang B, Pan J, Huang S, Wei Y, Ma H (2018) Simvastatin inhibits the development of radioresistant esophageal cancer cells by increasing the radiosensitivity and reversing EMT process via the PTEN-PI3K/AKT pathway. Exp Cell Res 362:362–369
29. Konge J, Leteurtre F, Goislard M, Biard D, Morel-Altmeyer S, Vaurijoux A, Gruel G, Chevillard S, Lebeau J (2018) Breast cancer stem cell-like cells generated during TGFβ-induced EMT are radioresistant. Oncotarget 9:23519–23531
30. Liu F, Zhang Y, Dong Y, Ning P, Zhang Y, Sun H, Li G (2021) Knockdown of AURKA sensitizes the efficacy of radiation in human colorectal cancer. Life Sci 271:119148
31. Shen ZT, Chen Y, Huang GC, Zhu XX, Wang R, Chen LB (2019) Aurora-a confers radioresistance in human hepatocellular carcinoma by activating NF-κB signaling pathway. BMC Cancer 19:1075
32. Liu JB, Hu L, Yang Z, Sun YU, Hoffman RM, Yi Z (2019) Aurora-A/NF-κB signaling is associated with radio-resistance in human lung adenocarcinoma. Anticancer Res 39:5991–5998
33. Guan Z, Wang XR, Zhu XF, Huang XF, Xu J, Wang LH, Wan XB, Long ZJ, Liu JN, Feng GK, Huang W, Zeng YX, Chen FJ, Liu Q (2007) Aurora-A, a negative prognostic marker, increases migration and decreases radiosensitivity in cancer cells. Cancer Res 67:10436–10444
34. Sun H, Wang Y, Wang Z, Meng J, Qi Z, Yang G (2014) Aurora-A controls cancer cell radio- and chemoresistance via ATM/Chk2-mediated DNA repair networks. BiochimBiophys Acta 1843:934–944
35. Oh ET, Byun MS, Lee H, Park MT, Jue DM, Lee CW, Lim BU, Park HJ (2010) Aurora-a contributes to radioresistance by increasing NF-kappaB DNA binding. Radiat Res 174:265–273

Figures

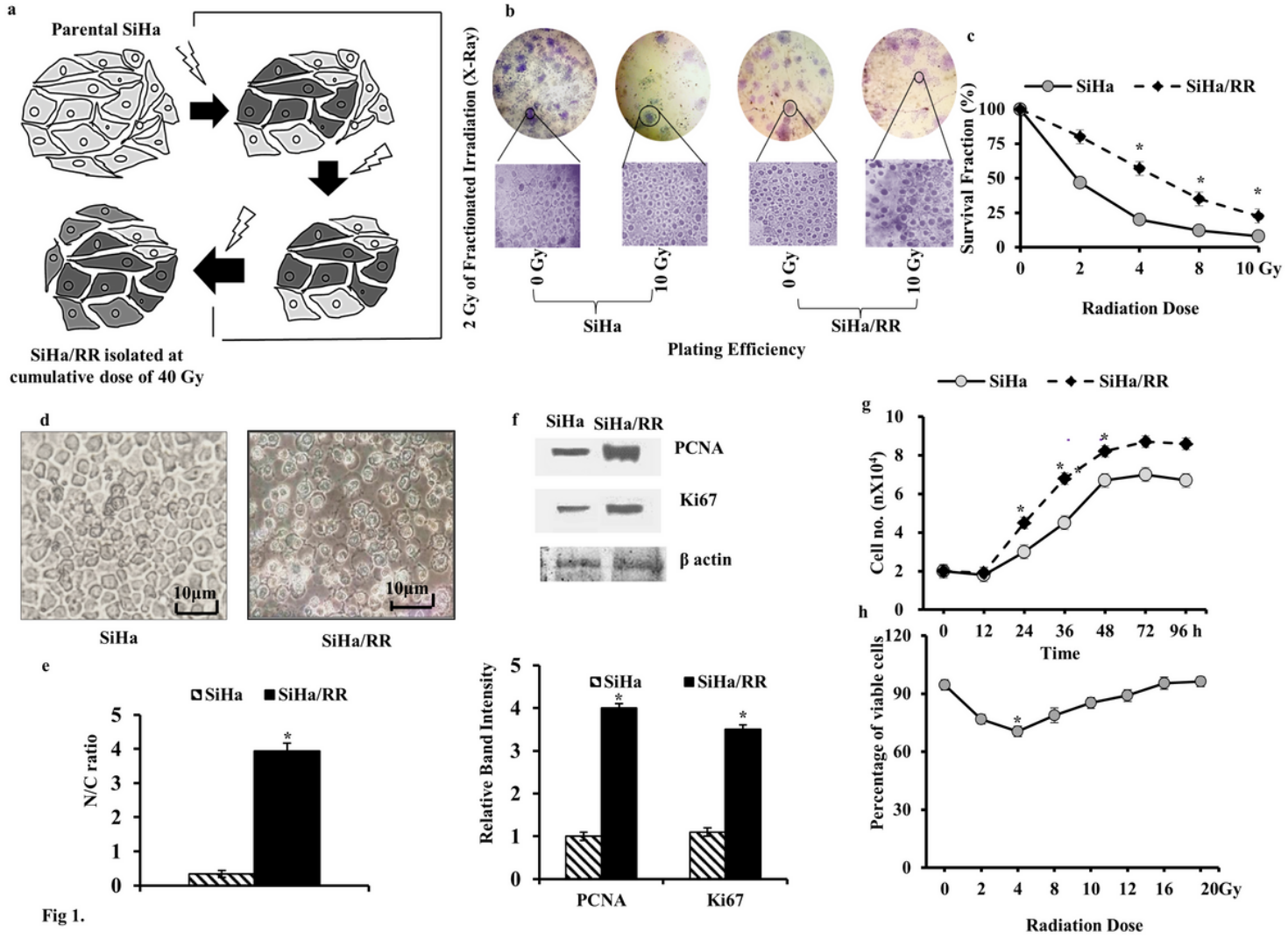

Figure 1

Characterization of radioresistant subline SiHa/RR, derived from parental cervical squamous cell line SiHa: a. Parental SiHa cells were exposed to weekly fractionated irradiation up to a total cumulative dose of 40 Gy. The radioresistant cell line as isolated was designated as SiHa/RR. b. Representative images of the colonies formed by SiHa and SiHa/RR cells in the presence and absence of exposure to 10Gy acute radiation. Window image magnification 400X c. Corresponding surviving fraction of cells subsequent to treatment with acute radiation. The values are mean ± SD of three independent experiments. d. Representative images as observed under Phase Contrast Microscope at 400X magnification; showing altered cellular morphology of SiHa/RR in comparison to SiHa. e. Corresponding calculated index of Nucleus:Cytoplasm. The values obtained are Mean ± SD of three independent experiments *p< 0.001. f. Western blot analysis of the expression levels of proliferative markers, (PCNA, Ki67) using β actin as loading control. Experiments were done in triplicate. Relative band intensities of PCNA, Ki67 were calculated and represented graphically to determine the fold increase (normalizing with loading control). The values obtained are Mean ± SD of three independent experiments, *p< 0.001. g. Time dependent increase in cell number of SiHa and SiHa/RR cells after exposure to acute dose of 10Gy; indicated

increased multiplication and proliferation rate of SiHa/RR cells relative to its parental cells. h. Graphical representations of viable cells upon staining with Typan Blue to exclude dead cells which became blue in colour. Percentage was calculated as No of live cells/ Total no of cells x100. Value obtained are Mean ± SD, *p< 0.001

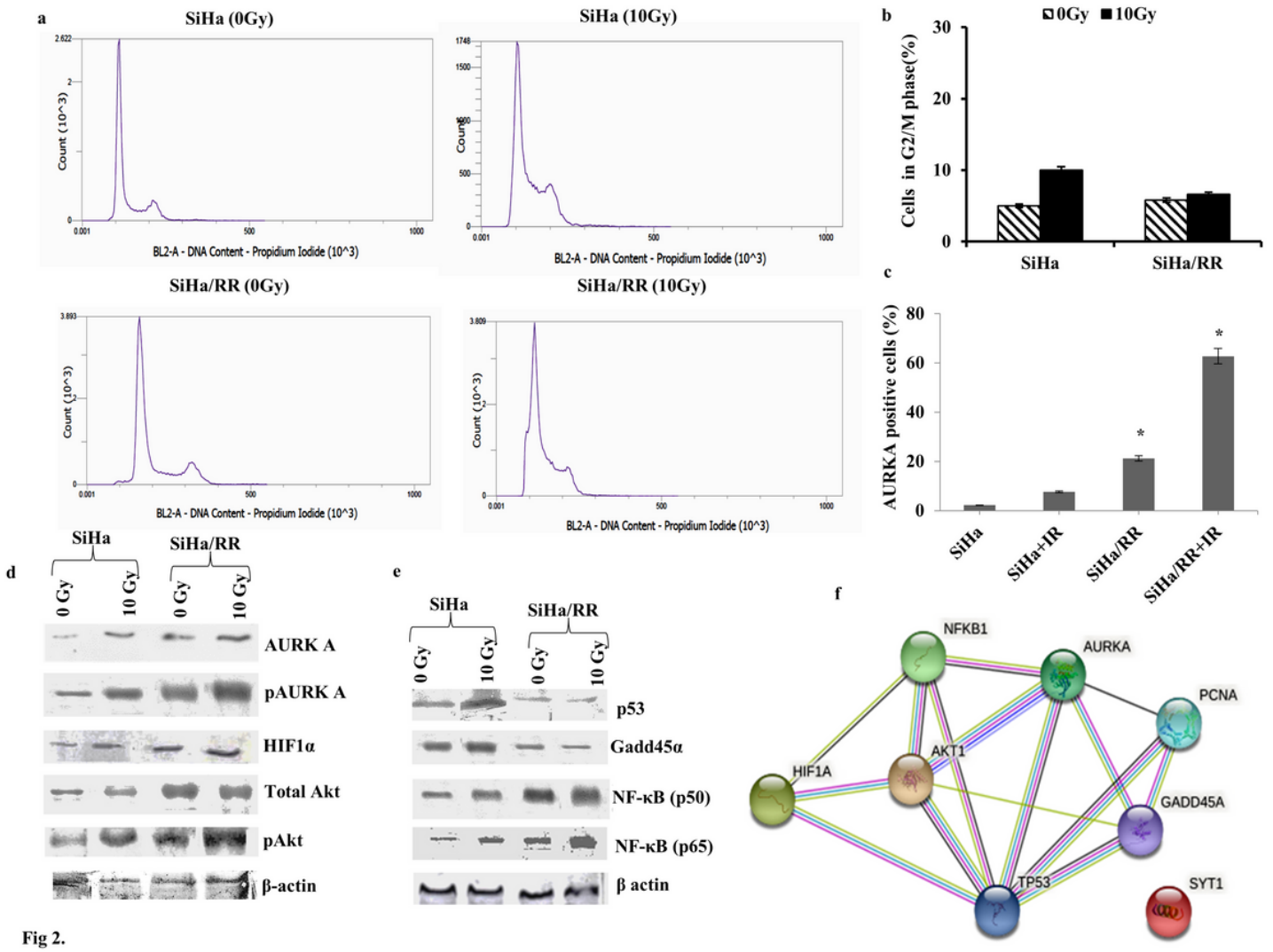

Fig 2.

Figure 2

Acquired radioresistant subline SiHa/RR escapes G2/M arrest by virtue of elevated AURKA level: a. Cell cycle distribution of radioresistant (SiHa/RR) and radiosensitive SiHa, exposed to acute dose of 10Gy radiation. Distribution of cells at different phases was measured by flow cytometry succeeding propidium iodide (PI) staining. b. Frequency distribution of cells at different phases of cell cycle shows that SiHa/RR has efficiently protected from radiation induced G2/M arrest. Data are represented as Mean ± SD. c. Flowcytometric analysis of AURKA expression in the cell population by immunostaining indicates a sharp rise in the expression of AURKA in SiHa/RR cells. All the experiments were independently repeated thrice, *p< 0.001. d. Parental and resistant cells subjected to western blotting using β-actin as loading control, showed elevated expression levels of AURKA, phospho AURKA, HIF1α, pAkt, total Akt, e. In a separate set of experiments expressions of effectors of AURKA (NF-κB p50/p65, p53 and Gadd45α) was carried out. β-

actin was used to ensure equal protein loading. f. Network based analysis of proteins to study their interactions with AURKA; showing close interactions among those proteins which have altered expression status in SiHa/RR.

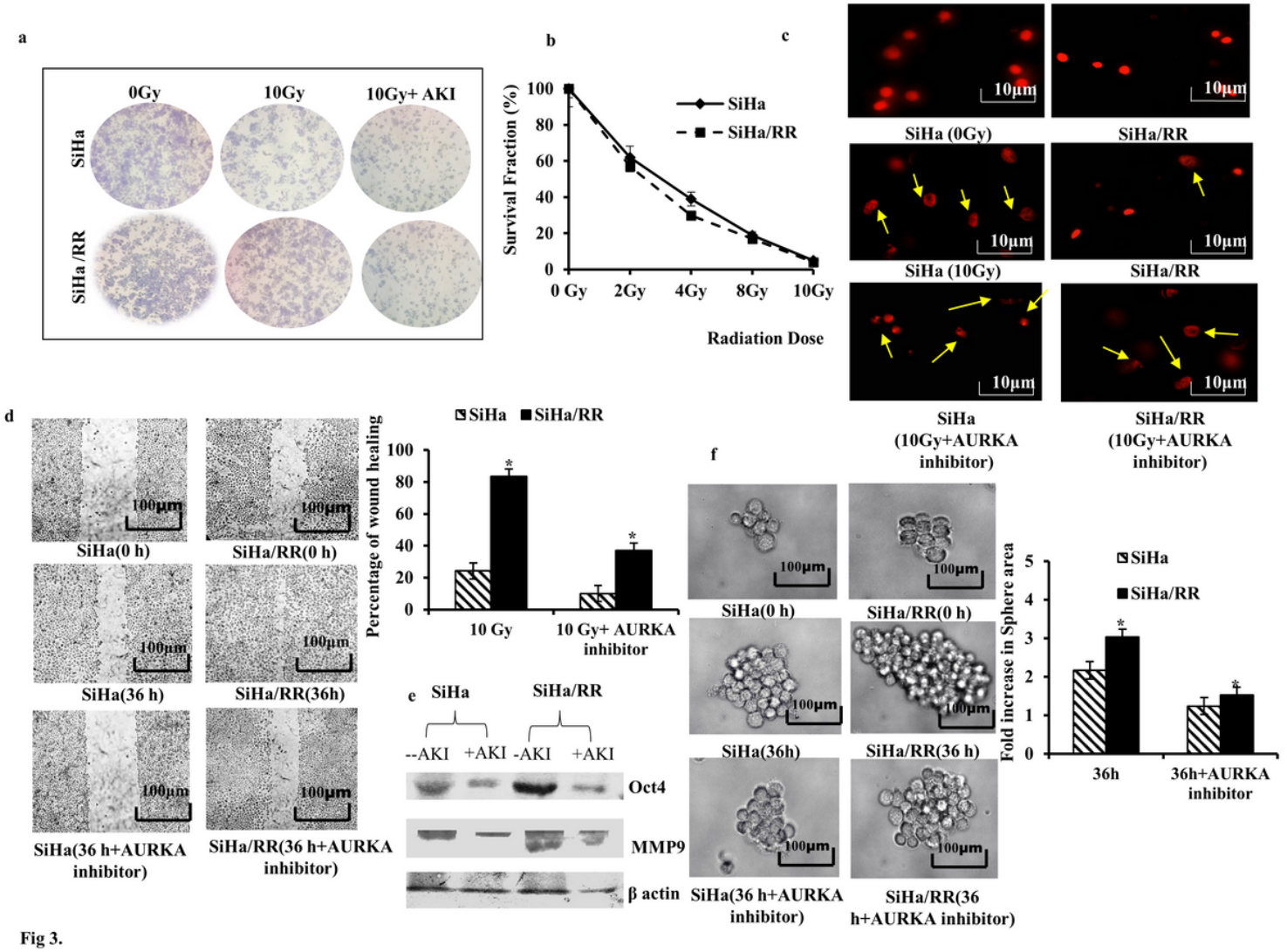

Fig 3.

Figure 3

AURKA inhibition restores radiosensitivity in SiHa/RR cells: a. SiHa and SiHa/RR cells were irradiated with an acute dose of 10Gy in the presence and absence of specific Aurora Kinase A Inhibitor I (AKI; 0.01 μM). Restrained colony forming ability was observed in SiHa/RR upon treatment with AKI. b. Survival fraction curves were plotted based on the number of colonies in the presence and absence of the AURKA inhibition. Values are Mean ±SD of three independent experiments. *p value is <0.0001 in respect to untreated cells. c. Ascertaining the apoptotic abilities of radioresistant cells upon treatment with AKI. Radioresistance was restored in those cells upon treatment with AKI. Apoptotic study of propidium iodide stained SiHa and SiHa/RR cells depicted increased apoptosis upon inhibition of AURKA. d. SiHa/RR showed decreased rate of wound closure ability upon treatment with AKI. Corresponding healing of wound healing was quantitated by calculating the wound area. The values represented Mean ± SD. e. Differential expression patterns of OCT4 and MMP9 proteins in SiHa and SiHa/RR cells exposed to10Gy

irradiation, prior to treatment with or without AKI; displays lower expressions of these EMT markers in SiHa/RR as a result of AURKA inhibition. f. Sphere forming ability of SiHa/RR was significantly reduced upon treatment with AKI. Relative fold changes of sphere area were calculated and as depicted from the graphical data, disclosed the downregulated growth of sphere area in SiHa/RR in the presence of AKI. All the experiments were repeated thrice and values were taken as Mean ± SD, *p< 0.001.

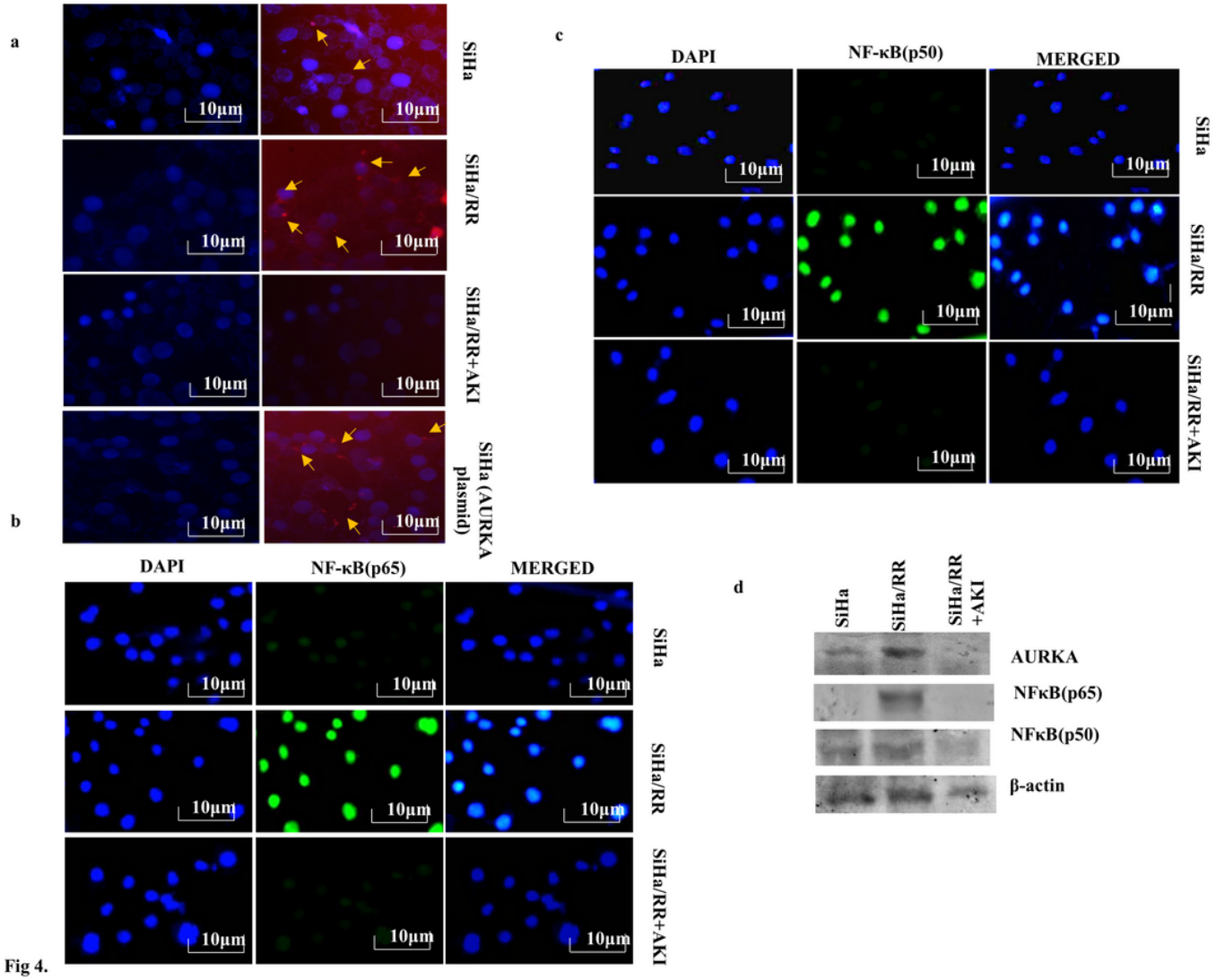

Fig 4.

Figure 4

Inhibition of AURKA blocks nuclear translocation of NF-κB in SiHa/RR cells: a. Intracellular localization of AURKA in SiHa and SiHa/RR cells (upper two panels). Immunostained cells showing altered localization of AURKA in SiHa/RR the presence of AKI (third panel) and increased intracellular localization of AURKA in SiHa upon ectopic overexpression of AURKA. b. SiHa/RR stained with NF-κB (p65) antibody also shows similar trends of regulated nuclear localization of the protein. Treatment with AKI (lower panel) justifies the involvement of AURKA in nuclear translocation of NF-κB (p65) in SiHa/RR. c. Immunofluorescent Staining of SiHa/RR with NF-κB (p50) in the presence and absence of AKI clearly indicates similar pattern of declined nuclear localization of p50 subunit upon AKI treatment. d. Western blot data showing reduction in the expression of NF-κB p50 and p65 protein isolated from the nuclear

extract of SiHa/RR as a result of AURKA inhibition. The findings are in coherence with IF data. The results are representative images of three independent experiments.

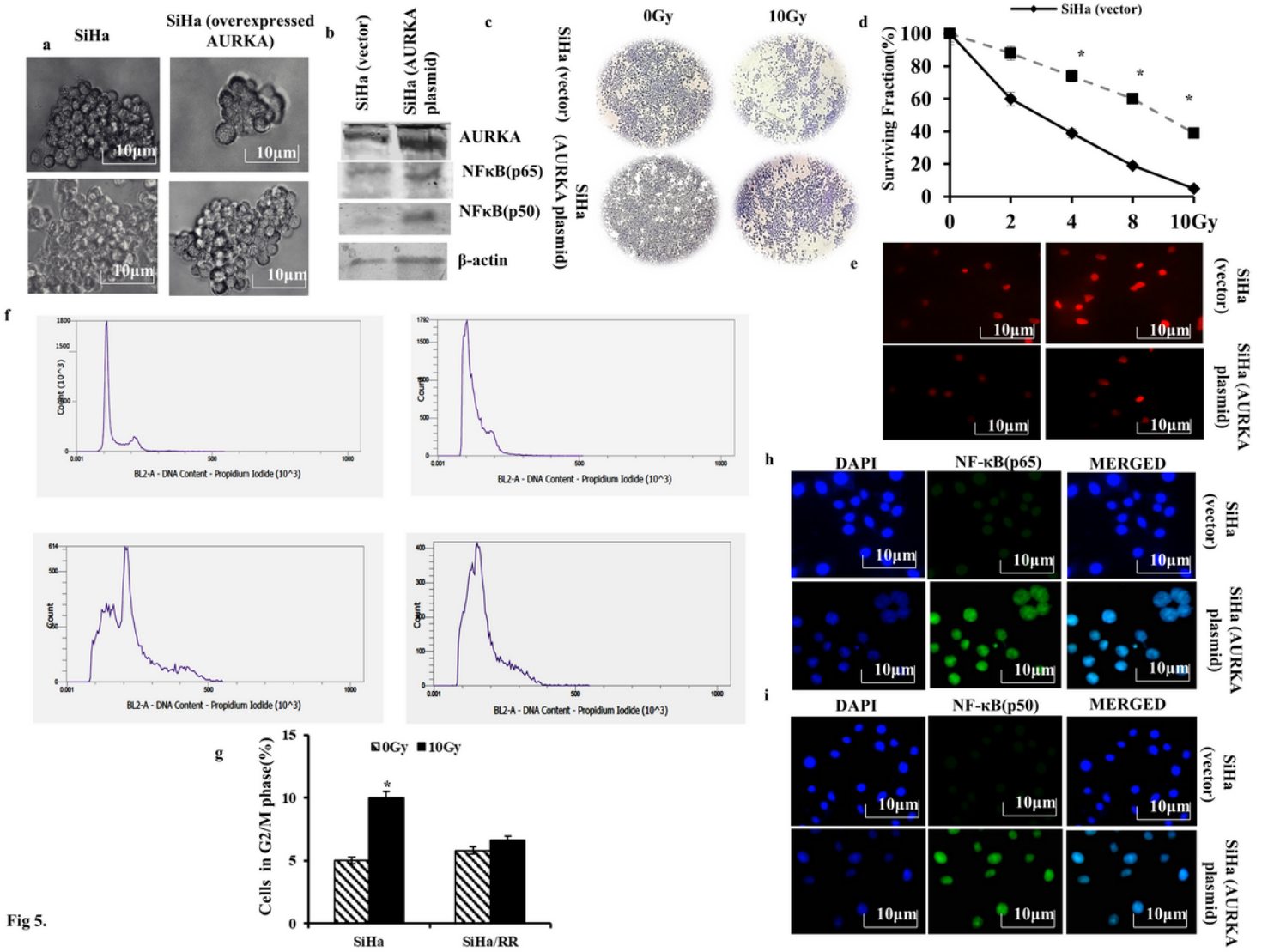

Fig 5.

Figure 5

Strengthening the role of AURKA in imparting radioresistance by ectopic overexpression in parental SiHa: a. Parental SiHa upon overexpression of AURKA shows better sphere forming abilities with enlarged sphere area compared to vector control SiHa. b. Western blot analysis of total (AURKA) and nuclear fraction NF-κB (p50) and NF-κB (p65); represents upregulated expression of these proteins in AURKA transfected cells. c. Clonogenic viability assay performed in SiHa cells in control and AURKA transfected cells, showed reduced radiosensitivity upon exposure to acute dose of 10Gy radiation. d. Graphical representation of survival fraction calculated on the basis of clonogenic assay showed higher survival fraction of SiHa in AURKA overexpressed condition, in response to 2, 4, 8, 10 Gy radiations. e. Radiation induced morphological features of apoptotic cells was observed under fluorescent microscope after staining vector control and AURKA transfected SiHa cells. Image magnification: 400X. f. Cell cycle phase specific distribution of SiHa (vector control vs AURKA transfected); showing altered ploidy in AURKA transfected cells g. Graphical representation showing cell cycle distribution pattern of SiHa (vector control

vs AURKA transfected). Each experiment was performed in triplicates and significance was determined by the value Mean ± SD, *p< 0.001. h. Increased nuclear localization of NF-κB (p65) in AURKA transfected cells as evident from Immunofluorescence using specific antibody of p65 subunit (Magnification: 400X). i. Elevated amount of NF-κB (p50) protein in the nucleus of ectopically overexpressed AURKA as observed under fluorescent microscope (Magnification: 400X).